

Mehta Raj Kumar  
Vijay Revonda

Department of Materials Engineering,  
Faculty of Engineering,  
University of Shukla,  
Shukla, INDIA

# Preparation of Zirconia Aerogel Nanostructures by Supercritical Drying Autoclave Method

*In this work, zirconium dioxide (ZrO<sub>2</sub>) aerogel monoliths were successfully prepared using drying autoclave method. The effects of synthesis environment on the morphological, optical and thermal properties of the synthesized monoliths were studied. The implemented autoclave was able to produce aerogel monolith of surface area up to 998.25 g/m<sup>2</sup> and thermal conductivity of 0.0053 mW.m<sup>-1</sup>.°C, associated with density of 0.047 g/cm<sup>3</sup>. It was found that the density, optical transmittance and porosity are strongly affected by the starting pH value as their final microstructures were introduced by scanning electron microscopy (SEM) and Brunauer-Emmett-Teller (BET) method. The lack of catalyst during aerogel preparation has resulted in dense, opaque and less porosity monoliths. As the environment was little basified, the aerogel properties were remarkably varied, while acidifying the reaction setting had gradual influence on the final aerogel properties. However, it is obviously requested for achieving desirable optically and nano-featured products.*

**Keywords:** Aerogel; Supercritical drying; Autoclave method; Nanostructures

## 1. Introduction

In the last decade, modifications on sol-gel method led to rapid progress in synthesis of porous structures and compounds. These structures and compounds are exceptionally important for different industrial, biological and environmental applications [1-3]. Zirconia aerogel has become very common when compared to other aerogel materials due to its interesting properties, mainly high specific surface area, high porosity, low thermal conductivity, low density and low refractive index [4-6]. Accordingly, many various applications of zirconia aerogel were recently presented [7,8].

In sol-gel method, nanostructured solid networks are formed in a liquid reaction media as a result of hydrolysis followed by polymerization processes creating O-Zr-O bridges between Zr atoms delivered by the precursor molecules, which is zirconyl chloride octahydrate (ZrOCl<sub>2</sub>·8H<sub>2</sub>O) [9,10]. The initial product of sol-gel process is the gel, where solvent will completely include the pores of gel. Then the solvent is removed from the gel by a drying step [11]. The main difficulty in drying gel is the occurrence of capillary forces in the pores due to surface tension of the liquid; where under conventional thermal drying the gel undergoes cracking and significant shrinkage (up to a few times its initial volume) [12]. Fundamentally, the fluids that full the pore volume are water as a result of condensation process and alcohol that adopted initially as well as by product of hydrolysis and condensation [13,14]. As a consequence of water have high surface tension compare with alcohols, therefore, we need to sock the gel several times by

pure alcohol prior to drying, and to pull water out resulted in alcogel, so that capillary forces will reduced [15]. Zirconia alcogel can be processed in some ways to yield aerogels and the route considered in this work is the production of the zirconia aerogel by supercritical drying method (SCD) [16,17]. By heating and compressing the gel above the critical temperature (T<sub>C</sub>) and pressure of its inner solvent, the solvent will be extracted from the gel without generating a two-phase system and hence the capillary forces will be minimized. In the final step, the alcogel inside the autoclave – under supercritical condition – must be cooled down and depressurized from critical point to the ambient condition. In this work, carbon dioxide (CO<sub>2</sub>) gas was used as the supercritical fluid [18,19].

## 2. Experimental Part

The chemicals used in the synthesis were, zirconyl chloride octahydrate (ZrOCl<sub>2</sub>·8H<sub>2</sub>O) abbreviated by ZOCW with purity >99.0%, ethyl alcohol (spectroscopic grade, 200 proof >99.5% purity), and deionized water catalyzed by ammonium fluoride (>98.0% purity). Deionized water was catalyzed by hydrochloric acid (0.15 M, >99.0% purity), and by ammonium hydroxide (28-30% concentration).

In order to construct the autoclave, a stainless steel tube of 18 cm diameter and 35 cm in length was used as a reaction chamber. This tube can be efficiently used for high-pressure purposes. High-quality valves were used to control the input and output flows through the chamber as well as to depressurize it. Tab heater and electronic-controlled

thermocouple were also used. Figure (1) shows the autoclave chamber used in this work.



Fig. (1) The autoclave chamber used in this work

The preparation of zirconia gels was consisting of a single-step procedure as follows. The zirconyl chloride octahydrate ( $ZrOCl_2 \cdot 8H_2O$ ), ethanol, water, and hydrochloric acid (or  $NH_4OH$ ) were mixed at molar ratio of 1:11:10:X, where X was varied to achieve sols of final pH value in the range 1 to 10. These sols were heated to 30 °C for 30 minutes in a magnetic stirrer. After that, a 0.5 ml of  $C_3H_7NO$  was added as a drying control chemical additive (DCCA) and kept for 60 minutes in the magnetic stirrer. The resulting sol was poured through a plastic tube of 24.5 mm in diameter and permitted to gelled and aged in the same tube for 28 hours at room temperature (27°C). The gel samples were rinsed with pure ethanol five times during 24 hours. Fresh ethanol was used for each successive step to remove any unreacted monomer that may residue from the gel network.

Zirconia aerogels were prepared using supercritical drying technique (low temperature carbon dioxide solvent exchange). Here, the alcogel is placed inside the autoclave as the sample be moisten at constant drenching with ethanol for 30 minutes. The autoclave was tightly closed and the  $CO_2$  gas was pumped into the autoclave very slowly until reaching pressure of 55 bars with the synchronization process of autoclave cooling to 5 °C until the liquid  $CO_2$  is obtained. This step will enhance the transfer of  $CO_2$  gas from gas into liquid state. The gel sample was separated from the liquid containing it inside the autoclave. These two liquids were kept stable for enough time then the liquid  $CO_2$  was changed more than 4 times for 28 hours to vent all undesired solvents out of the gel. This process makes the alcogel soaking just in  $CO_2$  liquid for further 36 hours. After that, heating process is started by slowly increasing the autoclave temperature using the wire heater to obtain supercritical condition at 73

bar and 32 °C. The temperature and pressure were maintained above the supercritical boundary to achieve the supercritical drying for 2-3 hours with depressurizing process every 30 minutes. Finally, depressurizing process will allowed to continue for few hours to get the zirconia aerogel with uniform shape. All prepared samples were finally kept in an oven at 700°C for one hour. The aerogel samples prepared at different pH values are shown in Fig. (2).

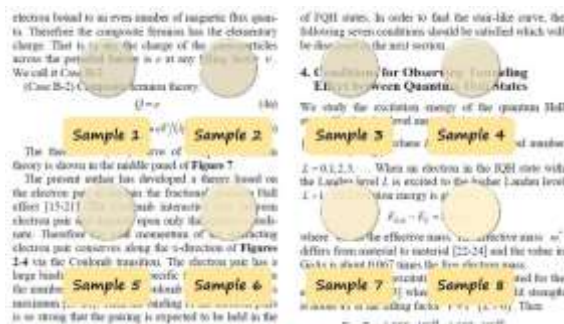


Fig. (2) Zirconia aerogel samples prepared at different pH values

Specific surface area and pore size of prepared aerogel were determined by the Brunauer-Emmett-Teller (BET) method using Micromeritics ASAP 2020 instrument. The microstructure and morphology of aerogel samples were introduced by scanning electron microscopy (SEM). The thermal conductivity of the prepared aerogel was recorded using Lee's disc apparatus. The spectral transmittance of the prepared aerogel was recorded by UV-visible spectrophotometer. By weighing cylindrical uniform aerogel samples of precise dimensions, the apparent densities were calculated. The dried aerogels were then annealed by heating up to 700 °C with a heating rate of 60 °C/hr.

### 3. Results and Discussion

The discussion was focused on three samples those may represent the acidic, neutral and basic environment as their pH values are 1, 7 and 8, respectively. They are denoted by pH1, pH7 and pH8, respectively. The transmittance spectra of the prepared zirconia aerogel in the entire visible region of these samples are shown in Fig. (3). It is clear that pH7, pH1 and pH8 samples exhibit lowest, moderate and highest values of transmittance, respectively.

The infrared (IR) transmittance spectra of the prepared aerogel samples are shown in Fig. (4). Several absorption bands are seen in these spectra. The formation of zirconia molecules was confirmed by two characteristic vibrational bands, a strong band centered at 460  $cm^{-1}$ , and another strong and broad band at 1104  $cm^{-1}$ . These bands are corresponding to the bending and asymmetric stretching vibrations of (Zr—O—Zr) groups, while the symmetric stretching characteristic zirconia band (O—Zr—O) is weak and seen at 812  $cm^{-1}$  [20,21]. A medium and broad band at 3500  $cm^{-1}$  and a small sharp band at 1650  $cm^{-1}$  are

ascribed to the vibration modes of O–H bond. These two bands confirm the existence of some residual (or adsorbed) free OH groups in the prepared aerogel samples [22,23].

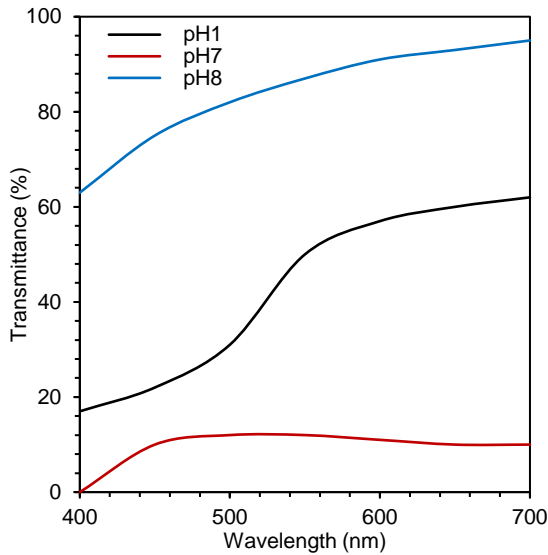


Fig. (3) Transmittance spectra for aerogel samples pH1, pH7 and pH8

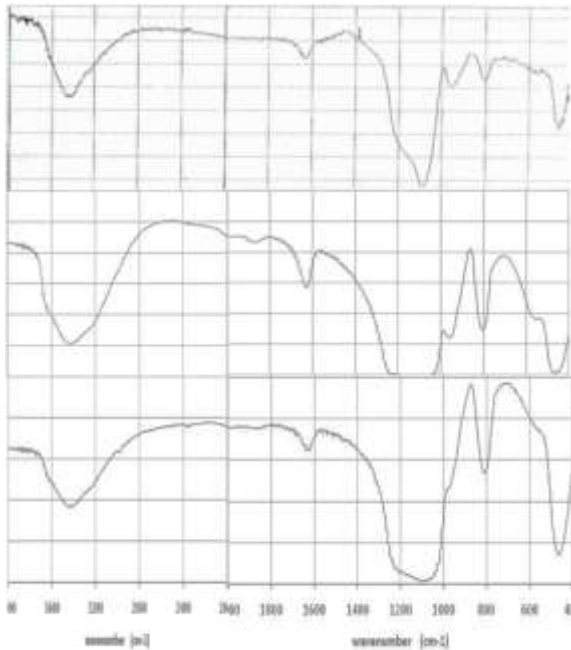


Fig. (4) FTIR transmission spectra for aerogels, pH1 sample (upper), pH7 sample (middle) and pH8 sample (lower)

The FTIR spectra for aerogel sample pH1 at three different annealing temperatures (500, 700 and 900°C) are presented in Fig. (5) while the linear isotherm plots for the aerogel samples prepared at several final pH values are shown in Fig. (6).

Table (1) shows the variation of thermal conductivity, density, transmittance at 550nm, surface area, pore volume, pore size and porosity with the final preparation pH value. Maximum pore size, pore volume and porosity were recorded for pH8

sample, while under neutral environmental, pH7, the product exhibit lowest pore size and volume as well as surface area.

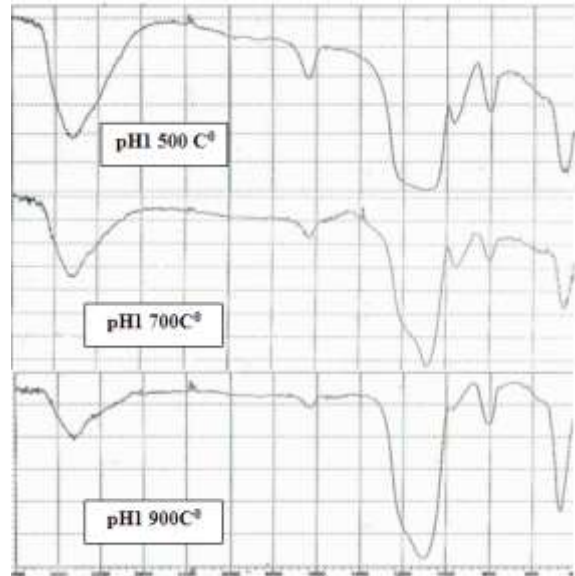


Fig. (5) FTIR spectra for aerogel sample pH1 at three different annealing temperatures (500 °C, 700 °C and 900 °C)

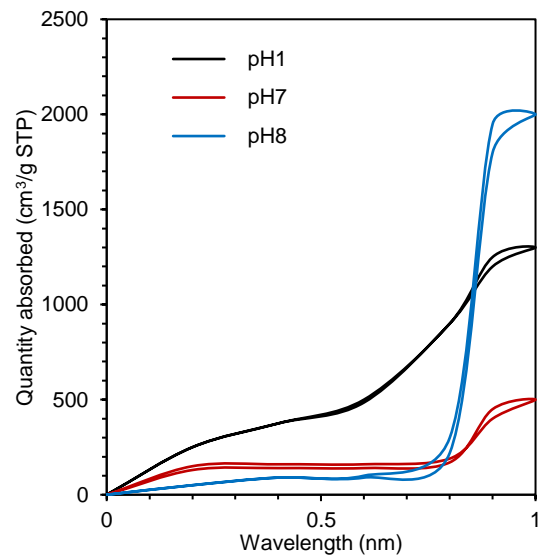
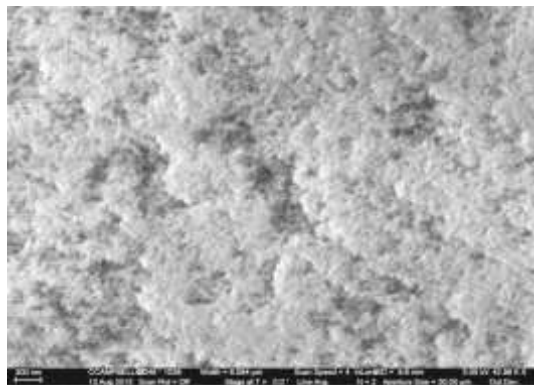


Fig. (6) Linear isotherm plot for three samples prepared at different pH values

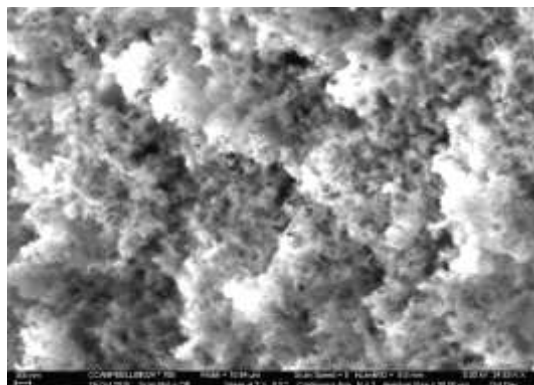
Table (1) Summary of properties and structural data of three samples prepared at different pH values

Sample	Surface area (m <sup>2</sup> /g)	Pore volume (cm <sup>3</sup> /g)	Pore size (Å)	Porosity (%)
PH 1	998.25	1.93	77.71	86.33
PH 7	102.19	0.11	44.91	43.76
PH 8	450.26	2.45	218.28	90.61
Sample	Thermal Conductivity (mW.m <sup>-1</sup> .°C)	Density (g/cm <sup>3</sup> )	T (%) @ 550nm	
PH 1	0.0063	0.051	50	
PH 7	0.016	0.129	6.8	
PH 8	0.0053	0.047	88	

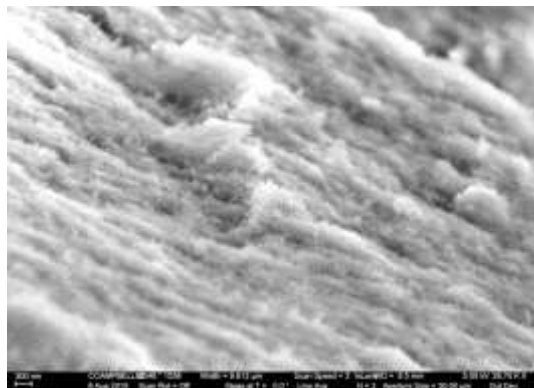
Figure (6) shows the SEM images for aerogel sample prepared in acid, base and natural environmental. It is obviously noted that the samples have different network structures related to their pH value. The morphology of these three samples is classified into distinct categories. The pH1 sample is monostructural characterized by a repetition of elongated open cellular foam microstructural features. The pH7 sample has very similar microstructure appears to be fractal in nature with a hierarchical repetition (similar shapes at different length scales). The microstructure of pH8 sample shows an isotropic ultrafine structure.



pH1



pH7

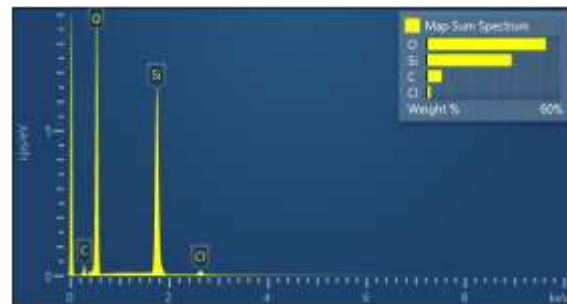


pH8

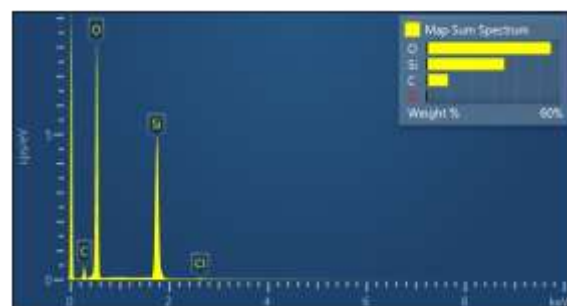
Fig. (6) SEM images for aerogel samples prepared at different values of pH

Excluding final pH values, the aerogels samples were prepared at the same conditions of reaction temperature, molar ratio (ZOCW: water) and aging time. Accordingly, the pH value was the exclusive varying factor affecting the aerogel microstructure, subsequently followed by other aerogel properties. Commonly, aerogels, as nanoporous materials, have highly transparency and low thermal conductivity [24]. However, acid and base catalysts have significant influence in this matter, where pH8 sample shows higher transmittance while lowest transmittance was shown at natural environment (pH7). Because the lowest reaction rate for hydrolysis occurs at pH=7 [25], many of zirconia networks still unreacted under this condition. Consequently, the electrophilic tendency of condensation terminates and the alcohol condensation mechanism becomes favorable [26,27]. This condition will give rise to more branchy networks, after a while leading to small pore volume and narrow pore size then to lowest transparency of pH7 (Fig. 3 and Table 1).

The EDS spectra shown in Fig. (7) are corresponding to the aerogel samples pH1 and pH7 before densification. They reflect the existence of residual alcohol carbon in pH7 sample, which is lower than that in pH1 sample.



pH1



pH7

Fig. (7) EDS spectra for aerogel samples prepared at different values of pH (pH1 and pH7)

The solubility of zirconia is reasonably low in the acidic environment (pH1), therefore, the formation and aggregation of primary particles of zirconia are coordinated as extremely building blocks of small primary particles correlated to high surface area of about 1000 m<sup>2</sup>/gm (see table 1). This reaction demands high electron density, therefore, the condensation process will result in more straight

chains. For pH8, condensed species are semi-ionized and therefore, mutually repulsive. Thus, the growth occurs primarily as a result of the addition of monomers to the more highly condensed particles rather than by particle aggregation [28,29]. This semi-ionized feature commonly gives rise to cracking tendency in the preparation of monolithic yielding size limitation. However, this can be overwhelmed using proper amount of DCCA. The transmittance was increased markedly in pH8 sample correlated with ultrafine structure at the nanoscale presented in the morphological SEM image.

Obviously, the FTIR spectroscopy is utilized for qualitative tests. In this work, the samples were prepared under appropriate standards, therefore, the relative amounts of bonds in the different samples can be compared to each other [30,31]. Zirconia aerogels often contain considerable amounts of adsorbed water appeared as a strong, broad band near  $3500\text{ cm}^{-1}$  and small sharp at  $1650\text{ cm}^{-1}$ . These two bands are ascribed to bending and stretching vibrations of O—H bond in  $\text{H}_2\text{O}$  molecules [32]. These bands are weakened by annealing at  $900\text{ }^\circ\text{C}$  as the intensities of these band were reduced but not vanished (Fig. 4 and 5). In fact, due to the hydrophilic tendency of zirconia aerogel prepared by supercritical method, the moisture may keep the O-H bond existing even if high temperature is used. Referring to figures (4) and (5), under basic environment, the fast condensation reactions have great chance to complete rather than slow reactions under neutral and acidic environments. Therefore, in case of preparation of optical elements from aerogels, considering anti-liquefaction as well as transparency requirements, it is strongly recommended to consider the preparation conditions of pH8 sample.

The weak band peak fixed at  $965\text{ cm}^{-1}$  may be ascribed to stretching vibration of zirconol ( $\text{Zr—OH}$ ) groups [23]. The intensity of this peak was decreasing monotonically with increasing annealing temperature. This may be due to the completion of the condensation reaction with temperature yielding more and more conversion of zirconol bonds to zirconoxane bonds ( $\text{Zr—O—Zr}$ ) [33].

The liner isotherm plots presented in Fig. (6) may confirm the above indications. The plots can be examined with the aid of the IUPAC classification hysteresis loops [34]. The hysteresis loops related to pH1 sample can be classified as H3 type which is correlated to non-rigid aggregates of plate-like particles (slit-shaped pores). In case of pH7 sample, the plot may be classified as H4 type which is linked to narrow slit pores including pores in the micropore region. Finally, the plot belonging to pH8 sample can be classified as H1 type, mentioned to well-defined cylindrical pore channels [35].

The lowest thermal conductivity was recorded for pH8 sample, the correlation between the porosity and thermal conductivity of zirconia aerogel as well as lowest density is clearly noticeable. In most cases, the

zirconia aerogel possesses very small (1-10%) three dimensional network fraction of solid zirconia. Therefore, the thermal transparent through the solid portion occurs through tortuous path [36].

## 5. Conclusions

A simple autoclave can used to prepare zirconia aerogel samples of proper physical properties. The structures and optical properties of such aerogels can be controlled by means of suitable selection of initial pH preparation value. Considering basic environment, highly transparent, lower density and crackly monoliths are prepared. On the other hand, using acidic catalyst, smaller particle size, higher surface area and more reactive aerogels are produced. Therefore, low-density thermal insulators, optical windows, and small-pore hydrogen storage tanks can utilize such aerogels by adjusting the starting catalyst.

## References

- [1] A. Amlouk et al., *Mater. Sci. Eng. B*, 146(1-3) (2008) 74-79.
- [2] C.M. Mo, Y.H. Li and Y.S. Liu, *J. Appl. Phys.*, 83(8) (1998) 4389.
- [3] D. Nakashima and R. Ikeda, *Phys. Rev. B*, 103(6) (2021) 064502.
- [4] E. Borsella et al., *Mater. Sci. Eng. B*, 79(1) (2001) 55-62.
- [5] E.E. Carpenter, *J. Appl. Phys.*, 99(8) (2006) 08N711.
- [6] F. De Nicola et al., *Phys. Rev. Appl.*, 14(2) (2020) 024022.
- [7] G. Zu et al., *Micropor. Mesopor. Mater.*, 238 (2017) 90-96.
- [8] H.H. Hamdeh and J.C. Ho, *J. Appl. Phys.*, 81(4) (1997) 1851.
- [9] J. Quintanilla, *J. Appl. Phys.*, 93(8) (2003) 4584.
- [10] J. Torres-Rodríguez et al., *J. Supercr. Fluids*, 149 (2019) 54-63.
- [11] K. Matsuzawa et al., *Mater. Sci. Eng. B*, 267 (2021) 115112.
- [12] K. Saravanan, B. Tyagi and H.C. Bajaj, *Appl. Catal. B*, 192 (2016) 161-170.
- [13] K. Shu et al., *Phys. Rev. B*, 104(5) (2021) L050801.
- [14] M. Liu et al., *J. Appl. Phys.*, 116(9) (2014) 093503.
- [15] M. Obori et al., *Phys. Rev. Appl.*, 11(2) (2019) 024044.
- [16] M. Qian, C. Xu and Y. Gao, *Mater. Sci. Eng. B*, 238-239 (2018) 146-154.
- [17] M.A. Worsley, J.H. Satcher Jr. and T.F. Baumann, *J. Appl. Phys.*, 105(8) (2009) 084316.
- [18] M.D. Guild et al., *Phys. Rev. Appl.*, 5(3) (2016) 034012.
- [19] M.D. Knudson and R.W. Lemke, *J. Appl. Phys.*, 114(5) (2013) 053510.
- [20] M.D. Knudson, J.R. Asay and C. Deeney, *J. Appl. Phys.*, 97(7) (2005) 073514.
- [21] M.-H. Jo et al., *J. Appl. Phys.*, 82(3) (1997) 1299.

- [22] P. Katanyoota et al., *Mater. Sci. Eng. B*, 167(1) (2010) 36-42.
- [23] P. Peshev et al, *Mater. Sci. Eng. B*, 97(1) (2003) 106-110.
- [24] P.E. Hopkins et al., *J. Appl. Phys.*, 111(11) (2012) 113532.
- [25] P.E. Stallworth et al., *J. Appl. Phys.*, 92(7) (2002) 3839.
- [26] R. Esquivel-Sirvent, *J. Appl. Phys.*, 102(3) (2007) 034307.
- [27] Rege, S. Aney and B. Milow, *Phys. Rev. B*, 103(4) (2021) 043001.
- [28] S.A. Bahrani, Y. Jannot and A. Degiovanni, *J. Appl. Phys.*, 116(14) (2014) 143509.
- [29] S.O. Kochev et al., *J. Appl. Phys.*, 101(12) (2007) 124315.
- [30] T. Coquil et al., *J. Appl. Phys.*, 106(3) (2009) 034910.
- [31] T. Hisamitsu and R. Ikeda, *Phys. Rev. B*, 103(17) (2021) 174503.
- [32] V.V. Dmitriev, A.A. Soldatov and A.N. Yudin, *Phys. Rev. B*, 120(7) (2018) 075301.
- [33] X. Lu, O. Nilsson and J. Fricke, *J. Appl. Phys.*, 73(2) (1992) 581.
- [34] Y. Kong, X. Shen and S. Cui, *Micropor. Mesopor. Mater.*, 236 (2016) 269-276.
- [35] Y. Lee et al., *Appl. Catal. A*, 506 (2015) 288-293.
- [36] Y. Zhang et al., *Mater. Sci. Eng. B*, 188 (2014) 13-19.
-